Polymer Blend Latex Films: Morphology and Transparency

Jianrong Feng and Mitchell A. Winnik*

Department of Chemistry and Erindale College, University of Toronto, Toronto, Canada M5S 1A1

Richard R. Shivers and Brian Clubb

Department of Zoology, University of Western Ontario, London, Ontario, Canada N6A 3K7

Received May 11, 1995; Revised Manuscript Received August 10, 1995[⊗]

ABSTRACT: Latex blend films were prepared from mixtures of two types of particles in dispersion, one composed of a high-T_g polymer [poly(methyl methacrylate), PMMA]; the other a copolymer of butyl methacrylate and butyl acrylate [P(BMA-*co*-BA)] with $T_g \leq 10$ °C. Transparent films were obtained under air-drying conditions if the PMMA particles had diameters less than ~250 nm and if the volume fraction of low-T_g latex polymer exceeded a certain critical fraction Φ_c. Values of Φ_c varied over a narrow range (0.40–0.50) with P(BMA-*co*-BA) particle size, and were independent of the T_g of the soft latex, ranging from ca. −35 to +10 °C. Film morphologies were examined by scanning electron microscopy and by freeze–fracture transmission electron microscopy. In all films, the hard particles retain their original size and spherical shape. In the transparent films, they are uniformly distributed in a polymer matrix generated from deformed soft particles, whereas clustering of PMMA microspheres is observed in turbid films. Various factors, such as increasing the size ratio between the two types of particles, removing of surfactant in the systems, and annealing of the films after drying, disrupt the uniform particle packing required for transparent films.

Introduction

Polymer blends have been the subject of study for many years. The fundamental driving force behind such investigations is the anticipation that in the blend one can obtain different properties than those of the individual components, and under some circumstances might even obtain unique properties.[1] Over this period of time there has been much less attention paid to latex blends. Such blends are prepared by mixing two polymers where each is present in the form of polymeric microspheres dispersed in a fluid medium. Blends prepared in this way would be expected, at least initially, to have a very high interfacial area. Upon aging or annealing, coalescence of adjacent latex with common composition will lead to coarsening of the morphology. The structures produced should be very different than the types of structures produced either through melt blending of the components or via phase separation of miscible blends.

One type of hybrid system which has come into prominence recently is that of latex-based impact modifiers for polymer resins.[2] In these systems, one blends a latex having a low glass transition temperature (or with a low-T_g core) with a high-T_g polymer. Such latex particles maintain their structural integrity within the matrix. They provide impact strength by intercepting crack propagation and by dissipating the energy of internal stresses into heat. In these blends, transparency can be achieved by balancing the indices of refraction of the core and shell components to match that of the matrix.

Latex Films. Interest in blends of two or more latex components has its origin in environmental issues pertinent to paint formulation. Environmentally friendly coatings are characterized by lower emission into the atmosphere of volatile organic compounds (VOC's). From this perspective, aqueous latex coatings are preferred over traditional solvent-based coatings. Nevertheless, latex paints themselves contain substantial quantities of volatile organic solvents.[3,4] These serve as promoters of coalescence and film formation.

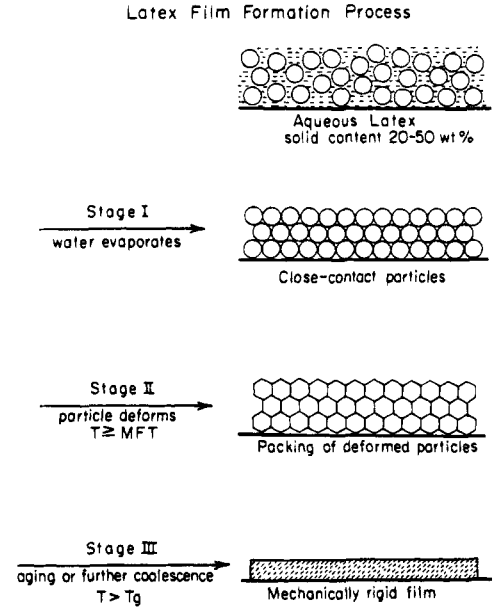

Figure 1. A simple representation of the latex film formation process.

To understand their function, one must look more closely at the film formation process. We depict the various stages in film formation in Figure 1. Initially the latex particles are present as a dispersion in water. As the water evaporates, the particles eventually come into contact. If the T_g of the latex in the presence of water is below room temperature (i.e., if the application temperature exceeds the minimum film forming temperature (MFT)), the particles will deform to produce space-filling Wigner–Seitz cells, yielding a transparent and void-free film. If the particles order into a face-centered cubic (fcc) array as they come into contact, the nascent film will be comprised of crystalline domains of essentially perfect rhombic dodecahedra. Such struc-

[⊗] Abstract published in *Advance ACS Abstracts,* October 1, 1995.

0024-9297/95/2228-7671$09.00/0

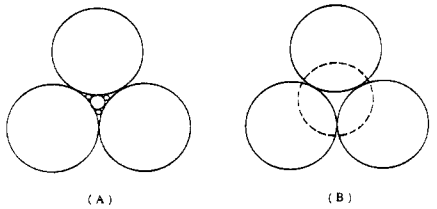

Figure 2. Particle arrangements in a blend to achieve high-density packing. When all particles are hard, the filler particles should have well-defined smaller sizes with respect to the voids that they are intended to fill, as shown in (A). When the filler particles are soft and deformable, their sizes need not be so rigorously defined. In (B), the smaller center particle (dashed circle) has exactly the volume needed to occupy the void among the close-packed larger particles.

tures can be seen by freeze–fracture transmission electron microscopy.[5,6] These nascent films are mechanically very weak. Mechanical strength develops over time or with annealing due to polymer diffusion across the particle–particle interfaces.[7,8]

Dispersions of low-T_g latex produce low-T_g films. These are tacky to the touch, and if two such surfaces are brought into contact, significant adhesion between them is observed. The ability to resist this adhesion is called "block resistance" in the coatings industry.[9] Good block resistance is one property of polymer films at temperatures well below their T_g. Historically, the strategy for producing high-T_g films from low-T_g latex has been to add organic solvents to the dispersion. Their role is to act as transient plasticizers, promoting both particle deformation during drying and healing of the interparticle interface during the early stages of film aging.[3,4,10] As they evaporate to the atmosphere, the T_g of the film increases, and block resistance develops.

At the current time there are no solvent-free latex paints available which also maintain the performance of traditional coatings. This is a classic problem, in which environmental issues require changes in product composition which initially leads to a decrease in performance. At the same time, these issues provide an opportunity for deeper investigation of the science behind the technology. One hopes that such investigations will provide the knowledge base for new materials with improved performance.

Strategies for Low-VOC Latex Coatings. There are several obvious strategies that one can imagine for producing latex films in the absence of volatile plasticizer. For example, one could use a reactive plasticizer that could polymerize or otherwise react to form nonvolatile products and at the same time raise the T_g of the system. Alternatively, one could develop latex with a surface region that could be plasticized by water. Here we consider a third strategy which is in fact common to the ceramics field. While no investigations of this type of latex blend film have been reported in the scientific literature, virtually every company in the coatings field has considered this strategy, which is also described in a recent European Patent application.[11]

The essence of this idea is that it recognizes two distinct contributions of film-forming additives to paint formulations. First, in plasticizing the latex, they decrease the modulus and promote particle deformability. Second, by increasing free volume in the system, they promote polymer diffusion across the interparticle boundary. In the ceramics field, one also has to produce solid objects by fusing particles. Sintering large particles requires significant deformation and flow. To minimize the need for large-scale deformation, one can try to mix large and small particles in such a way that the small particles fill the interstitial spaces between the larger particles. Because all the particles are so hard to deform, strategies for ceramics place strict demands on the relative sizes of the different particles and their arrangement in the system. These requirements are shown in Figure 2A. In latex blend films, one can use mixtures of a hard latex and a soft latex. The low-T_g latex should deform under the conditions of film formation, i.e., evaporation of water, while the high-T_g latex becomes incorporated into the matrix. Under these circumstances, the size of the soft latex may still be a factor but may not be very important. In Figure 2B we depict a latex mixture in which the soft latex has exactly the volume needed to fill the interstitial spaces of a randomly close-packed array of hard spheres.

To test these ideas, we have synthesized hard and soft latex particles of various sizes and soft particles with a range of T_g values. From mixtures of these dispersions, films were prepared and examined for transparency. Selected films in the transparent and opaque regions of the phase diagram were further studied by scanning and transmission electron microscopy (SEM, TEM) to investigate their respective morphologies. In the following sections we provide details of sample preparation and describe the results of our measurements.

Table 1. Recipe for Preparation of 110 nm PMMA Latex

first stage		second stage	
MMA (mL)	10.5	MMA (mL)	86
water (mL)	135	PheMMA (g)	2.5
KPS (g)	0.12	[or AnMA (g)	2.4]
SDS (g)	0.30	water (mL)	75
$NaHCO_3$ (g)	0.12	KPS (g)	0.12
		SDS (g)	1.80
temp (°C)	80	temp (°C)	80
time (h)	1	time (h)	20

Experimental Section

Materials. The monomers, including methyl methacrylate (MMA, Fluka, 99%), butyl methacrylate (BMA, Aldrich, 99%) and butyl acrylate (BA, Aldrich, 99%), were distilled under reduced pressure under a nitrogen atmosphere and kept in a refrigerator before use. Deionized and double-distilled water was used in emulsion polymerization. The initiator, potassium persulfate (KPS, Aldrich, 99%), surfactant, sodium dodecyl sulfate (SDS, Aldrich, 98%), and buffer, sodium bicarbonate (Caledon, 99%), were used as supplied.

Preparation of Latex Dispersions. All emulsion polymerizations were carried out under a nitrogen atmosphere. The hard latex samples are composed of poly(methyl methacrylate) (PMMA). These were prepared by semibatch emulsion polymerization of MMA, involving two stages of polymerization. In the cases where fluorescent labeling of the polymer particles is needed, a fluorescent comonomer, either (9-phenanthryl)methyl methacrylate (PheMMA) or 9-anthryl methacrylate (AnMA), was incorporated into the monomer feed in the second stage. A three-neck round glass flask, equipped with a mechanical stirrer, a condenser, and a nitrogen inlet, was used for the polymerization. In the seed stage, all the ingredients were mixed before heating except that the initiator was added when the reaction mixture had reached the desired temperature. In the second stage, the monomer solution and the aqueous solution of the initiator and surfactant were both fed into the reactor continuously at a slow rate (e.g., 0.05 mL/min) by use of metering pumps. The particle size was controlled primarily by the amount of surfactant used in the emulsion polymerization, and all samples had a narrow size distribution. The recipe for preparing 110 nm diameter particles is shown in Table 1. Other samples of PMMA latex had diameters in the range of 45–400 nm.

Table 2. Recipes for Preparation of P(BMA-*co*-BA) Latex

	sample								
	III-1-1	III-1-4	III-1-5	III-1-6	III-1-7	III-1-8	III-1-9	III-1-10[a]	III-1-11[b]
					Batch Stage				
BMA (mL)	3.5	2	0	1	2	0	5	2	2
BA (mL)	3.5	0	2	1	0.5	0	1.2	0.5	0.5
water (mL)	100	100	100	100	100	500	500	485	485
KPS (g)	0.085	0.085	0.085	0.085	0.085	0.425	0.425	0.30	0.30
SDS (g)	0.44	0.44	0.44	0.33	0.33	1.65	1.65	0.66	0.66
$NaHCO_3$ (g)	0.09	0.09	0.09	0.09	0.09	0.45	0.45	0.45	0.45
temp (°C)	70	70	70	70	70	70	70	70	70
time (h)	1	2	2	2	2	0	1	1	1
					Semibatch Stage				
BMA (mL)						2.0	10	13	13
BA (mL)						0.5	2.55	3.25	3.25
AnMA (g)								0.32	
PheMMA g)									0.32
water (mL)								15	15
KPS (mL)								0.15	0.15
SDS (g)								1.0	1.0
temp (°C)						70	70	70	70
time (h)						4	4	4	4

[a] An-labeled. [b] Phe-labeled.

The soft latex samples are composed of poly(butyl methacrylate-*co*-butyl acrylate) [P(BMA-*co*-BA)]. These copolymer latex samples were prepared by both batch and semibatch emulsion polymerizations. These smaller-sized particles were obtained by increasing the surfactant concentration along with decreasing the monomer concentration in the polymerization systems. In this way we were able to obtain dispersions with particle diameters ranging from ca. 20 to 55 nm. The recipes for preparation of these P(BMA-*co*-BA) latex samples are summarized in Table 2.

In some cases, latex dispersions were cleaned by the ion exchange method to remove surfactant and other ionic substances before film formation. Before use, the mixed bed ion exchange resin (Bio-Rad, AG-501-X8) was washed sequentially with hot deionized water (~85 °C), deionized water, methanol, and then deionized water until the last wash water had the same conductivity as the pure water, as suggested by Vanderhoff.[12,13] The washed resin was then added to a dilute latex dispersion (solid content 1–3 wt %), using 3–5 g of resin for every 100 mL of solution. The mixture was magnetically stirred at room temperature for 40–60 min. The resin was separated from the dispersion by filtering with glass wool. This process was repeated three times with each sample.[14] The latex dispersion was finally concentrated to 10 wt % solids by rotary evaporation.

Latex Characterization. Particle size and size distribution were determined by dynamic light scattering using a Brookhaven BI-90 particle sizer. Some of the PMMA samples were also examined by scanning electron microscopy (SEM). The solid content of each dispersion was determined gravimetrically. Glass transition temperatures (T_g) of the latex polymers were measured with a Perkin-Elmer differential scanning calorimeter (DSC-7) at a heating rate of 10 °C/min and under a N_2 atmosphere. Molecular weights were determined by gel permeation chromatography in THF on freeze-dried latex samples, using PMMA standards to calibrate the columns.

Film Formation and Characterization. A weighed quantity of P(BMA-*co*-BA) latex was mixed with a certain amount of PMMA latex and agitated for several minutes. A Pasteur pipet was used to suck in and squeeze out the liquid several times to let the dispersion be sufficiently mixed. The mixed dispersion, having a solid content of ca. 10 wt %, was then coated onto a glass or quartz substrate and allowed to dry at room temperature. In most cases, the substrate with the dispersion was covered with an inverted Petri dish to slow down the water evaporation rate throughout the drying process. The dried films have a thickness of 30–50 μm.

Film transparency for each sample was measured with a UV–vis spectrometer (Hewlett-Packard 8452A Diode Array). The film was mounted in front of the sample window of the spectrometer, and its transmittance (T%) was scanned in the visible range (400–700 nm). When comparing the transparency for a set of samples, the T% values were recorded at 550 nm. We note that one could easily distinguish by eye a transparent film from a turbid film.

Film morphologies were examined both by scanning electron microscopy (SEM) and by freeze–fracture transmission electron microscopy (FFTEM). Prior to the SEM measurements, films were coated with a layer of gold onto their surfaces to prevent charging of the films and to slow down the melting of soft polymer under the electron beam. To study the internal morphology, FFTEM measurements were carried out. Latex films were prepared on polystyrene plastic cover slips as the substrate. The plastic surface was rendered wettable by dipping it into a 1 wt % aqueous solution of poly(styrene-*b*-ethylene oxide) block copolymer and allowing it to dry. These films were then sent to the University of Western Ontario for FFTEM measurements. The basic procedure for further sample treatment and fracture replication has been described elsewhere.[6]

Results

Experimental Design. We began this project with the idea that the relative size of the soft latex compared to the hard latex would be important in producing transparent and void-free films. As suggested in Figure 2, the original idea was to match the size of the low-T_g latex to the void volume ($\Phi_v = 0.34$) of randomly close-packed spheres. Since the two materials would have somewhat different indices of refraction, achieving transparency should require that the hard latex be small with respect to the wavelength of visible light. Thus our initial target was to prepare PMMA microspheres with a diameter of ca. 100 nm, which is quite straightforward, and to prepare low-T_g latex much smaller in size, which is much more difficult.

As the soft latex material, we chose to examine copolymers of butyl methacrylate and butyl acrylate. By varying the ratio of butyl methacrylate (BMA) to butyl acrylate (BA) in the emulsion polymerization, a series of latex samples with various T_g values were obtained. The samples prepared have T_g values in the dried state, as determined by DSC, ranging from −33 to +10 °C. Because of the chemical composition differences between the low-T_g copolymer and the PMMA latex, we anticipate very little miscibility or chain interpenetration at the hard latex–soft matrix interface in the latex films.

Table 3. PMMA Latex Characteristics

	sample					
	PMMA				PhePMMA	AnPMMA
diameter (nm)	44	110	230	400	107	109
polydispersity	0.005	0.005	0.005	0.005	0.005	0.005
solid content (wt %)	7.2	31.0	23.3	7.9	31.2	30.0
M_w ($\times 10^{-5}$)	4.6	3.7			2.1	2.1
M_w/M_n	2.0	2.3			2.3	3.1
labeling (mol %)					1.0	1.0

Interface thickness can in principle be determined by nonradiative energy transfer measurements in films in which the PMMA latex and soft latex are labeled, respectively, with donor and acceptor groups. Since we anticipate carrying out such experiments, several of the materials described here were synthesized in such a way that they contain a small amount of a fluorescent group covalently bound to the polymer. To prepare small-diameter soft latex particles, significant amounts of surfactant had to be used in the synthesis. In some experiments, this surfactant is carried forward into the films. Other experiments use latex previously cleaned by ion exchange to remove the surfactant and other ionic substances in the dispersion. The preparation of these various materials is described in the Experimental section, and a list of these materials and their properties is collected in Tables 3 and 4. The particle size and size distribution listed in the tables were evaluated by dynamic light scattering.

Film Transparency. Films were prepared on substrates by air-drying the dispersions. Once dried, they were inspected by eye for turbidity or opaqueness, and then the percent transmittance of all films was measured by UV–vis spectroscopy. In some instances, the dried films were annealed at temperatures just below the T_g of PMMA, and some films were annealed at 140 °C, well above the T_g of PMMA. The T_g measured for PMMA was 105 °C.

For the film samples which were transparent to the eye, UV–vis measurements indicate that the transmittance is on the order of 85–95% within the scanned wavelength range, while for the samples noted as turbid films, the transmittance is only 5–20%, as shown in Figure 3. An important feature of a transparent film is that there are negligible voids remaining in the film, which can scatter light.[4] This requires complete coalescence of particles for the latex system. In our binary latex system, the hard particles are not able to deform; therefore it is essential that the soft particles we chose can deform and serve as a binder for the hard particles.

Two other criteria for transparency in a polymer blend film are that the refractive indices of the two polymers must be similar, as pointed out by Bohn,[15] and that the dispersed domain sizes must be small, as pointed out

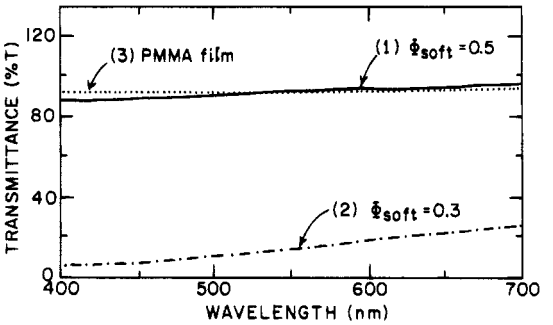

Figure 3. Visible transmittance spectrum of (1) a clear latex blend film, (2) a turbid latex blend film, and (3) a solvent-cast PMMA film. The two latex blend films contain PMMA hard particles of d = 110 nm and soft particles of d = 55 nm and T_g = 5.1 °C. The volume fractions of soft polymer in the films are (1) 0.5 and (2) 0.3, respectively.

by Rosen.[16] Refractive indices for PMMA, PBMA, and PBA homopolymers are 1.490, 1.483, and 1.474,[17] respectively. These values are reasonably close and may be one reason that our films composed of well dispersed PMMA and P(BMA-*co*-BA) have good optical clarity. As we will see when we examine micrographs of these films, turbidity is associated with aggregation of the hard latex. Thus the issue we address in this paper concerns the conditions necessary to obtain well-dispersed hard particles in the film matrix. Our first important observation is that film transparency depends mainly on two factors, film preparation conditions and blend composition.

Preparing transparent films from these latex blends requires proper external conditions during film drying. These include temperature, humidity, air flow speed, and the film thickness and surface area. These parameters will affect the rate of water evaporation and particle deformation. A certain time is required for the soft particles to deform to fill the void spaces in the film. We found that when the blend dispersions were dried too fast, only turbid films were obtained. For example, when the dispersions were dried at room temperature with rapid air flow generated by a fan in an oven, the drying took about 1.5–2 h and led to turbid or translucent films. When we elevated the film formation temperature (e.g., to 40 °C), the drying time was shortened to 1–1.5 h, and only turbid films were formed. Most of the films to be described below were formed at room temperature and with a slow water evaporation rate by covering each dispersion with an inverted Petri dish. It took about 15–20 h for the films to form and dry in this way. Note that our latex samples were often quite dilute (solid content 5–15%) and thus required longer drying times than more concentrated dispersions. Clear films can also be obtained in the open air in the laboratory free from draft, with a drying time of 5–10 h. We also observed that the latex blends dried at

Table 4. P(BMA-*co*-BA) Latex Characteristics

	sample								
	III-1-1	III-1-4	III-1-5	III-1-6	III-1-7	III-1-8	III-1-9	III-1-10[b]	III-1-11[c]
diameter (nm)	43	25	28	28	32	21	38	49	55
polydispersity	0.008	0.042	0.088	0.018	0.026	0.13	0.017	0.077	0.082
solid content (wt %)	6.16	2.27	2.37	1.82	2.57	2.58	2.78	3.62	3.78
conversion (%)	94.0	96.2	100	75	96.0	96.5	94.0	96.0	100
T_g[a] (°C)	−33.0	22.9	−55	−33.8	−6.9	−1.9	4.1	9.9	5.1
M_w ($\times 10^{-5}$)	8.4	2.8			6.7	1.3	3.5	1.1	5.1
M_w/M_n	1.7	2.1			1.9	3.0	24	6.9	5.5
labeling (mol %)								1.0	1.0

[a] Only one T_g was observed by DSC for each copolymer sample. [b] An-labeled. [c] Phe-labeled.

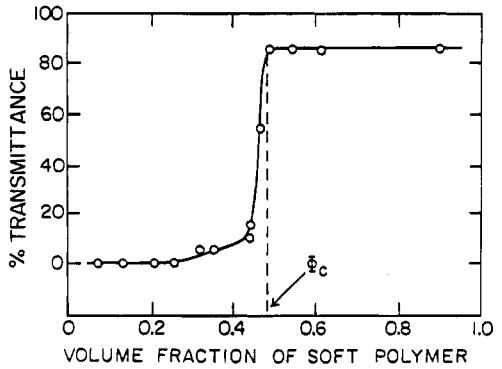

Figure 4. An example of the change of optical clarity of latex blend film samples with increasing volume fraction of soft polymer. The dashed line represents our definition of the critical volume fraction of soft polymer, Φ_c, for formation of a clear film. This set of films was prepared by mixing soft particles having d = 38 nm (T_g = 4.1 °C) with hard particles of d = 110 nm.

significantly slower rates than corresponding dispersions of the soft latex component alone. This aspect will be described in more detail in a future publication.

Other important parameters for film transparency include the choice of both the particle sizes and the T_g of the latex polymers. In blends, one would also expect that the blending ratio of the two components should determine the film properties. We will discuss these issues in the following paragraphs.

Volume Fraction of Soft Polymer. If the hard spheres undergo no deformation, one might expect that the volume fraction of soft polymer necessary to give transparent films would correspond to that necessary to fill the void volume in the close-packed hard spheres. This volume fraction Φ_{soft} would be equal to 0.26 or 0.34 depending upon whether the close packing was face-centered cubic or random. In all the examples we studied, for the 50 and 110 nm PMMA microspheres mixed with each of the various soft particles having T_g of 10 °C or lower and a diameter in the range of 20–55 nm, we found that there is a value of the volume fraction of soft polymer at which we could obtain a clear film and below which we only could get a turbid film with cracks or, in the extreme, a white powder. We define this as the critical volume fraction of soft polymer, Φ_c, in these blend films

$$\Phi_{soft} = V_{soft}/V_{total}$$

$$\Phi_c = (V_{soft}/V_{total})_c$$

where the volume of each polymer was calculated from its known weight and density. The density of PMMA is 1.19 g/cm^3.[17] Since the densities of pure PBMA and PBA are very close, 1.06 and 1.08 g/cm^3,[17] respectively, we take the value of 1.06 g/cm^3 as the density of our soft copolymer consisting of PBMA as a major component.

Figure 4 shows an example of the change of film transmittance with increasing P(BMA-*co*-BA) component. From this phase diagram, we define Φ_c as the endpoint of the sharp transition range from turbid to clear in the sample. The transition is so sharp that we could as well have chosen the midpoint of the transition as the value of the critical composition. Since Φ_c is an important parameter for characterizing for film formation from binary or multicomponent latex systems, it is interesting to examine how other factors, such as the

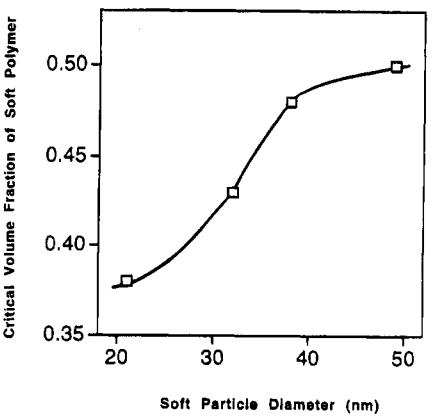

Figure 5. Variation of Φ_c with increasing diameter of the soft latex from 20 to 50 nm. Here the PMMA latex is 110 nm in diameter.

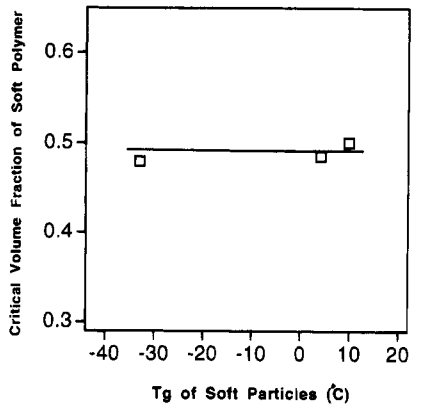

Figure 6. Φ_c values for the film samples consisting of soft particles having T_g of −33, 4.1, and +9.9 °C and diameter of 43, 38, and 49 nm, respectively. Here the PMMA latex is 110 nm in diameter.

size of particles, the size ratio of hard particles to soft particles, and the T_g of the soft polymer, affect Φ_c values.

When hard particles of constant size (110 nm) are mixed with different sized soft particles (20–50 nm in diameter), Φ_c increases with increasing soft particle size, as shown in Figure 5. However, the change of Φ_c occurs over a very small range (0.38–0.50), indicating relatively little dependence of size ratio on the Φ_c value. This can be understood after one has more knowledge of the packing state of the particles in each film. This will be discussed in more detail below.

When hard particles of constant size (110 nm) are mixed with soft particles with different T_g values (in the range of −33 to +10.0 °C), Φ_c values do not change significantly. Examples of Φ_c values for the film samples having T_g of soft particles of −33, +4.1, and +9.9 °C, respectively, are shown in Figure 6. Normally, film-forming conditions are strongly dependent on the T_g of the polymer, which is a reflection of the MFT of the dispersion. This result may imply that the randomness of particle packing is similar when the types of soft particles used have different deformation and flow ability. Decreasing T_g of the soft particles may promote the fusion (autohesion) between the soft particles but does not affect the Φ_c values.

Transparent films could also be obtained with 230 nm diameter PMMA latex, but not with 400 or 560 nm particles.

Surfactant Effects. It is well known that in latex coatings, surfactant affects the film formation process, film microstructure, and film properties.[3,4,6] According

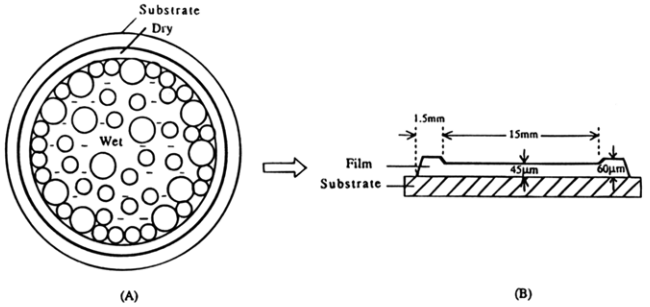

Figure 7. (A) A representation of a moving-front drying process where drying occurs from the edge to the center, showing a transparent dry region at the edge separated by a wet region in the center. A major part of the central region having a lower particle density and a particle-rich region near the edge would exist. (B) Films produced from surfactant-containing dispersions have a thick rim surrounding a flat center. A cross-section view of this kind of film is shown, accompanied by the dimensions of one such film obtained here.

to our observations, the film drying process for surfactant-containing latex is not uniform from edge to center. Initially, the dispersion spreads spontaneously over the flat glass substrate and forms a convex layer. The drying process occurs as a moving front from edge to center. On the outer side of the front (edge), the drying occurs more quickly and the particles come into irreversible close contact with each other in a relatively short time. On the inner side of the front (near the center), the latex is present as a colloidal dispersion. Upon further drying, the front moves toward the center of the film and separates a transparent dry region from a turbid moist region. Additional time is required for the drying of the central region, and finally a clear film is formed. This process is illustrated in Figure 7.

Interestingly, these films always have an edge thicker than the flat central region. An example of such a kind of film dimensions is shown in Figure 7B. Here the small portion at the film edge has the thickness of 60 μm and the flat part of the film center is 45 μm thick. This difference in thickness is even larger (e.g., 80 versus 40 μm) in some film samples.

When the surfactant is removed from the dispersion, the drying also occurs as a moving front but the drying front propagates at a relatively slower rate. The resultant films have much more uniform thickness over the surface area than the corresponding surfactant-containing samples.

Film Morphologies. (a) Surface Morphology As Seen by SEM. Clear films can be obtained from each of our soft latex dispersions. An example of a SEM image of these films is shown in Figure 8. We see from this image that a continuous film is formed from these soft particles (d = 55 nm). On the film surface there are many nonspherical granules with sizes ranging from 300 nm to 1 μm. These kinds of granules are seen in films formed from surfactant-containing dispersions, including those formed from binary particle systems. No such objects appear in films prepared from latex dispersions cleaned to remove surfactant. Therefore we identify these granules as crystals of SDS surfactant exuded to the surface during the film formation process.

In these soft latex films, the amount of surfactant is rather high (6−15 wt %). This large amount is the result of the high ratio of surfactant to monomer needed to prepare small latex particles. When we produced films using this kind of dispersion mixed with the dispersion of hard particles, the weight of total ionic surfactant to polymer is in the range of 4−8 wt %. From

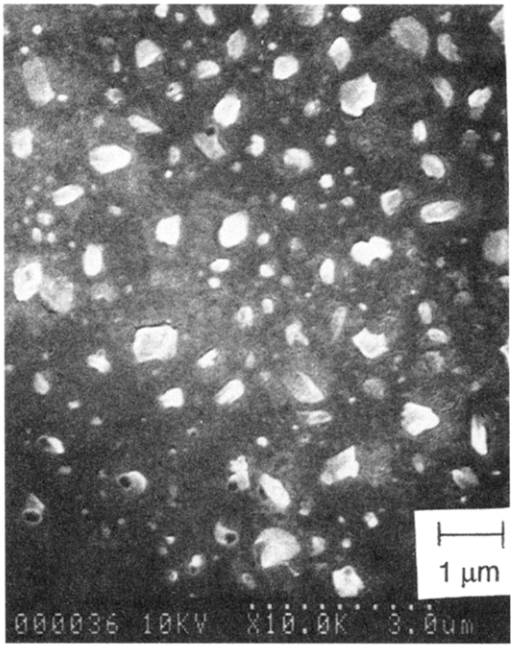

Figure 8. An image of surfactant-containing soft latex film. This film was prepared from a sample with d = 55 nm (T_g = 5.1 °C). The SDS content in the film is ca. 8.8 wt %, and the solid objects seen at the film surface are thought to be surfactant crystals.

another point of view, there is a significant interest in the fate of surfactant in latex films.[18−20]

The presence of surfactant crystals on the surface often makes it difficult for us to see the hard particles in films formed from binary particle dispersions. Nevertheless, observations can be made since these crystals differ both in size and in shape from the hard particles. Typical packing patterns for transparent films composed of about 1:1 volume ratio of hard to soft components are presented in Figure 9. In Figure 9A, the hard particles have a diameter of 110 nm and the soft particles have a d = 55 nm and T_g = 5.1 °C. In this sample, the hard spheres seem to be randomly distributed and embedded in the continuous phase generated by the soft latex. Figure 9B is an image of a transparent film containing 230 nm hard particles and soft particles having a T_g of 9.9 °C and d = 49 nm. A similar result (Figure 9C) is obtained for a film comprised of a 1:1 mixture of 44 nm hard particles and 43 nm soft latex, which give a highly transparent film. Once again, at the surface, the hard particles are randomly distributed in the continuous film. The cracks seen in the SEM image are caused by electron beam damage.

There is a tendency for the hard particles to aggregate in these films. In films comprised of 400 nm diameter PMMA latex, clear regions and turbid domains are apparent to the eye. In the SEM, no PMMA spheres are seen in certain regions of the film (not shown), which we are tempted to associate with the transparent domains, whereas aggregates are clearly apparent in other domains (Figure 10) which likely are turbid. Aggregates are also seen in turbid films obtained from smaller PMMA latex (e.g., 230 nm).

To examine the effects of surfactant, another set of films was prepared using dispersions consisting of a mixture of hard and soft particles which were first carefully cleaned by ion exchange to remove the surfactant. Clear films were obtained from mixtures of 110 nm diameter hard latex with a wide variety of soft particles, having diameters of 20−55 nm and T_g's in the

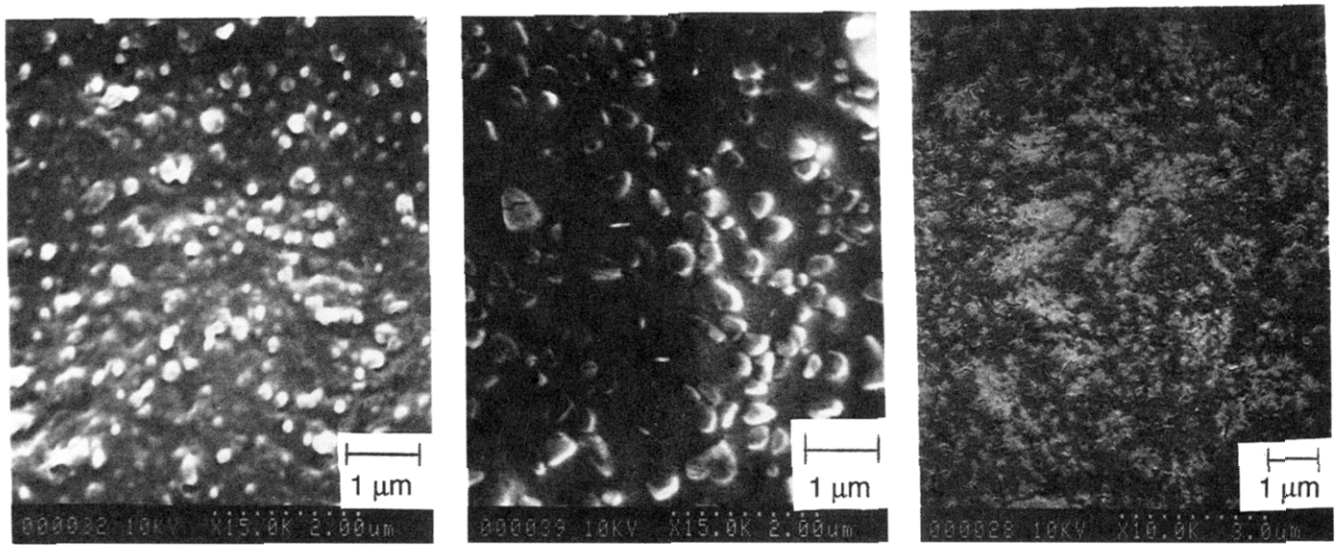

Figure 9. SEM images of the pattern of random distribution of hard particles seen in transparent latex blend films. The sizes and size ratios (D_{hard}/D_{soft}) and T_g of the soft particles ($T_{g,soft}$) for the samples are (A) D_{hard}/D_{soft} = 110 nm/55 nm and $T_{g,soft}$ = 5.1 °C, (B) D_{hard}/D_{soft} = 230 nm/49 nm and $T_{g,soft}$ = 9.9 °C, and (C) D_{hard}/D_{soft} = 44 nm/43 nm and $T_{g,soft}$ = −33 °C. The volume ratios of hard to soft components in these samples are all about 1:1.

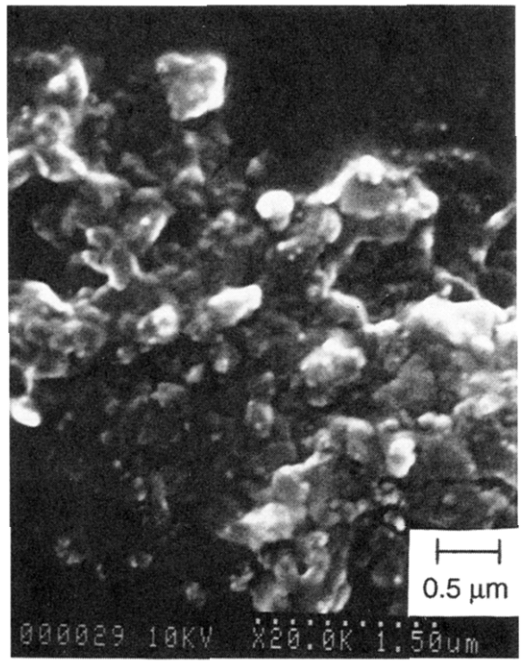

Figure 10. A SEM image showing clustering in a latex blend film containing hard particles 400 nm in diameter.

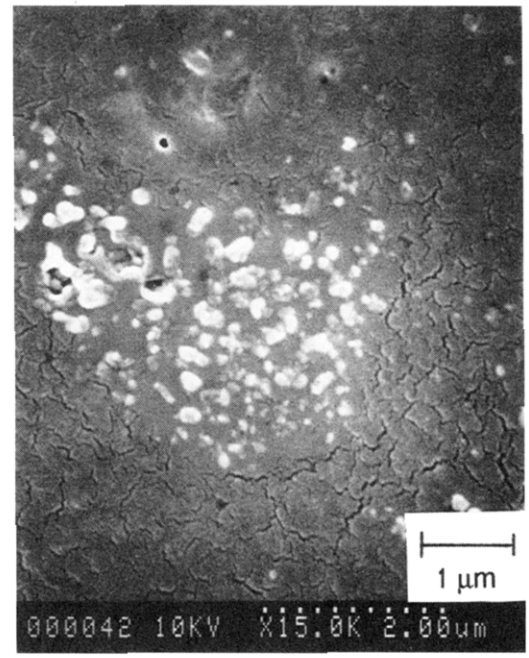

Figure 11. A SEM image of a blend film prepared from a surfactant-free dispersion comprised of 110 nm hard particles. D_{soft} = 49 nm, V_{hard}/V_{soft} = 1, and $T_{g,soft}$ = 9.9 °C.

range −33 to +10 °C. Film formation conditions for these mixtures and values of Φ_c are very similar to those for the surfactant-containing dispersions. The SEM image in Figure 11 shows that on the surface of one such film there is a region containing a high concentration of hard particles separated by a soft-polymer-rich region. Since these films exhibit good optical clarity, the association of hard particles at the surface is not sufficient to cause significant turbidity.

When analogous films were prepared from 230 nm diameter PMMA latex, two different types of results were obtained. Depending on the characteristics of the soft particles used, some films obtained were clear and some films were merely translucent. Figure 12A is an image of a film of D_{hard}/D_{soft} = 230 nm/49 nm, V_{soft}/V_{hard} = 1, and the T_g of the soft polymer = 9.9 °C. In this image we see that there are three kinds of regions on the film surface, a deformed soft particle region, a region containing individually distributed hard particles, and a region where the hard particles seem to be joined together, probably caused by bridging of hard particles with soft polymer. These films are clear (*T*% up to 85%). The bridging of particles seen on the film surface may reflect a certain amount of particle association in the original dispersion because of the absence of surfactant. When a soft latex having a very low T_g (−33 °C) and a similar size (43 nm) was mixed with the 230 nm hard particles with V_{soft}/V_{hard} = 1, only turbid films were obtained (*T*% = 20−30%). From the SEM, we can see that here large clusters of hard particles exist on the surface, and one such aggregate is shown in Figure 12B. This film has a different appearance and a different

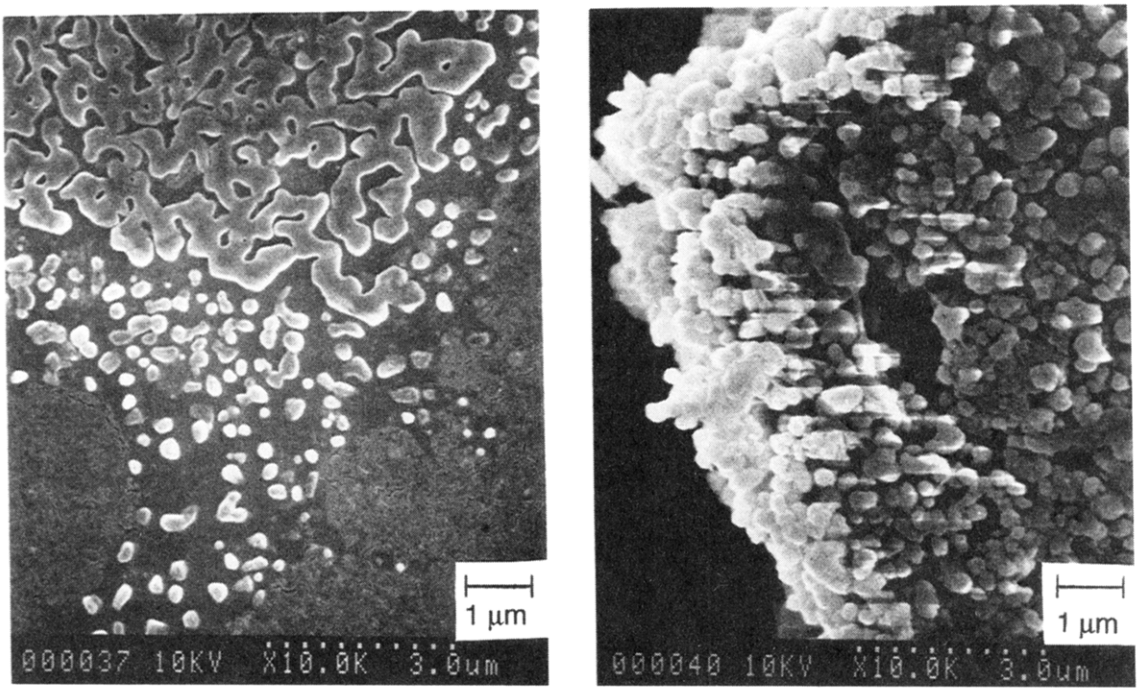

(A) (B)

Figure 12. SEM images of surfactant-free blend films consisting of 230 nm hard particles, showing different kinds of particle packing. Film A is transparent whereas film B is turbid. These samples were prepared using (A) $D_{soft} = 49$ nm, $V_{hard}/V_{soft} = 1$, and $T_{g,soft} = 9.9$ °C and (B) $D_{soft} = 43$ nm, $V_{hard}/V_{soft} = 1$, and $T_{g,soft} = -33$ °C.

morphology than the corresponding film prepared from the surfactant-containing dispersion. This is our first indication that the removal of surfactant can favor the clustering of the hard latex in the course of drying.

(b) Internal Morphology As Seen by FFTEM. A limited number of film samples (all containing surfactant) were examined by FFTEM experiments. This technique provides a rich view with high resolution of the fracture surface of the film interior. Fracturing is carried out at low temperature (−110 °C) in a frozen aqueous glycerol matrix to minimize fracture-induced distortions of the morphology. In Figure 13, we show FFTEM images for three films consisting of a 1:1 mixture of 110 nm PMMA particles plus soft latex, with the T_g of the latter ranging from −33 to +5 °C. We see that the morphologies are essentially similar. The hard (PMMA) particles preserve their spherical form, and the size calculated from the image is consistent with that determined for the particles in dispersion by dynamic light scattering. These hard particles are very uniformly distributed in the soft polymer matrix. The T_g of the soft polymer affects the rate of fusion of the soft particles but does not significantly influence the distribution of hard particles in the matrix.

In Figure 14 we examine the influence of particle size and size ratio on the internal film morphology. For these 1:1 mixtures, very uniform mixtures are obtained irrespective of the size of the low-T_g latex (21−55 nm) or the size of the small PMMA microspheres. The particle diameter ratio in these films varies by a factor of 5. A similar image is obtained in the case of transparent films comprised of 230 nm PMMA. Close inspection of these images reveals the presence of smooth patches ranging in size from 50 nm to several hundred nanometers. Previous work in our laboratory provided strong evidence that these patches are due to surfactant crystals in the film.[6]

Discussion

In our systems, we were often able to obtain transparent films from binary mixtures of PMMA latex with smaller low-T_g P(BMA-*co*-BA) microspheres. In these films, the PMMA particles remained spherical and dispersed in the continuous matrix generated from soft particles. The soft particles serve as a binder. The size of the low-T_g latex plays only a small role in determining whether transparent films will be formed. Substantial deformation of these particles leads to flow sufficient to fill in all the interstitial spaces in the film. Our view of the morphology for our films in relation to transparency is shown in Figure 15.

The formation of transparent films is ultimately governed by a phase diagram. Dispersions which contain an excess of hard particles do not form transparent films. Φ_c is an important parameter for characterizing film formation from binary or multicomponent latex systems. Like MFT, it reflects the film-forming ability of the system. Φ_c shows a slight increase with increasing soft particle size, as shown in Figure 5. This suggests that when the soft particles are smaller, they can more efficiently fill the interstitial spaces between the hard particles. However, the change of Φ_c occurs over a very small range (0.38−0.50), indicating relatively little dependence of size ratio on the Φ_c value. It also seems that Φ_c is not sensitive to the T_g of the soft particles used, provided that the randomness of particle distribution in the final film is not significantly influenced by the polymer composition in the particles.

Particle Interaction in the Fluid State. According to the model of the mechanism of latex film formation presented in Figure 1, all particles move about through Brownian motion during the evolution of the

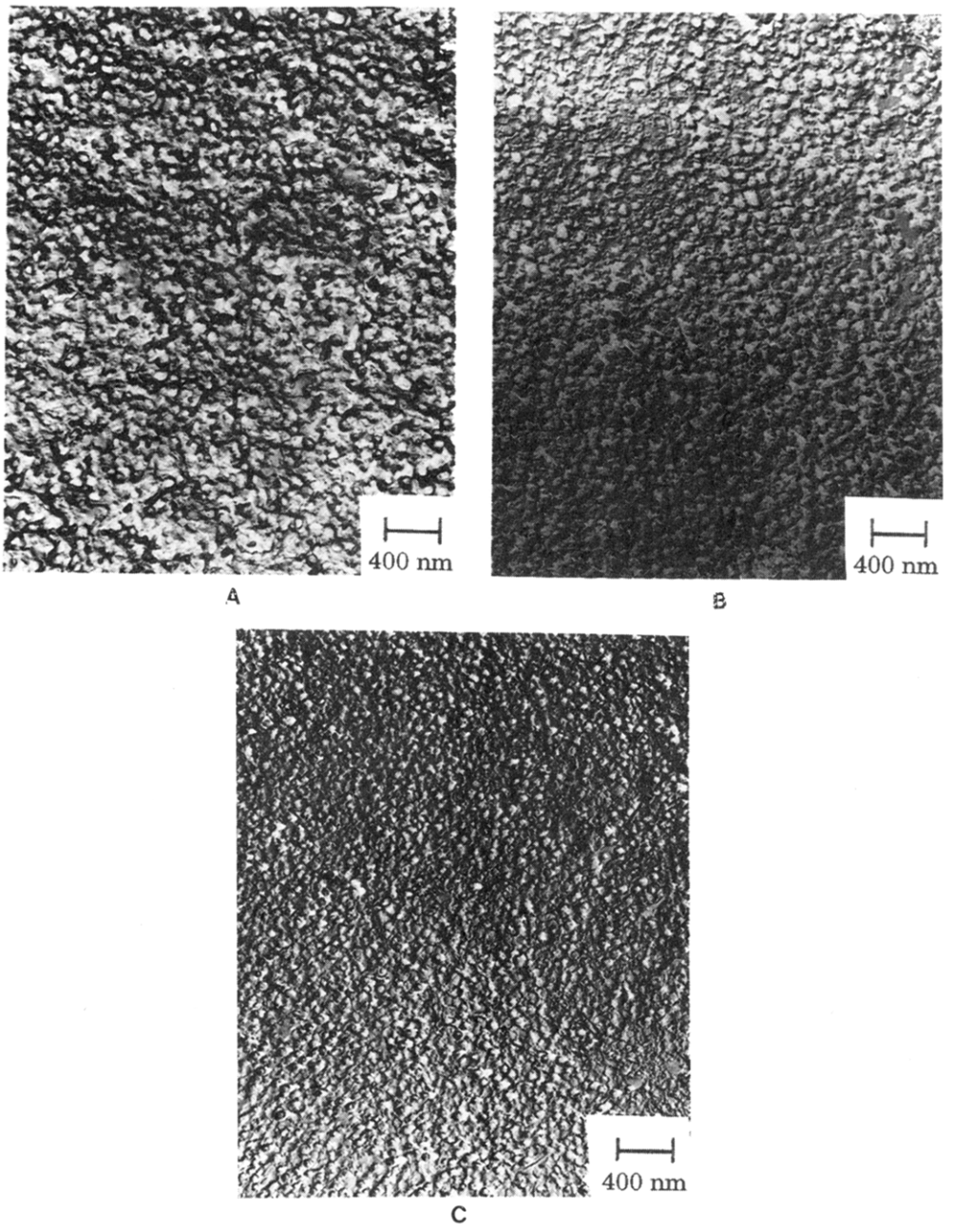

Figure 13. FFTEM images of transparent latex blend films of 1:1 mixtures of 110 nm PMMA particles and soft particles having T_g of (A) −33, (B) −6.9, and (C) +5.1 °C, respectively. The corresponding soft particle sizes in these samples were 43, 32, and 55 nm in diameter, respectively.

system from dispersion to particle contact. Given sufficient time, the particles will arrange themselves in a way that makes possible the most compact packing. The way particle interactions affect packing may change as the concentration increases due to further evaporation of water. Henson, Taber, and Bradford[21] reported that in a film formed from polydispersed latex, large globules are surrounded by small globules. In their view, this particle packing state was generated when the particles came into irreversible contact with one another. No matter how the subsequent coalescence between particles took place, the morphology of the film was derived from the particle packing in the first stage. This nature of this state in the concentrated dispersion should relate primarily to the colloidal properties of the particles (e.g., surface characteristics) and only indirectly to the polymer composition of the particle.

It would be useful in understanding the generation of film morphology to have information about the distribution of particles in binary colloidal mixtures. Israelachvili has commented, for example, that there is always an effective attraction between particles of the same species in a binary mixture.[22] In addition, following up on ideas presented by Denkov et al.,[23] one would also like to know how packing in a mixture is affected by the flow fields created by evaporation of water in the system. Some information on particle distribution in colloidal mixtures has recently become available.

Bartlett and Ottewill[24] used small angle neutron scattering (SANS) to examine colloidal dispersions composed of mixtures of particles of different sizes. We note that their colloidal systems are different from our latex dispersions, in both the choice of particles and the type of medium. For their system they point out that

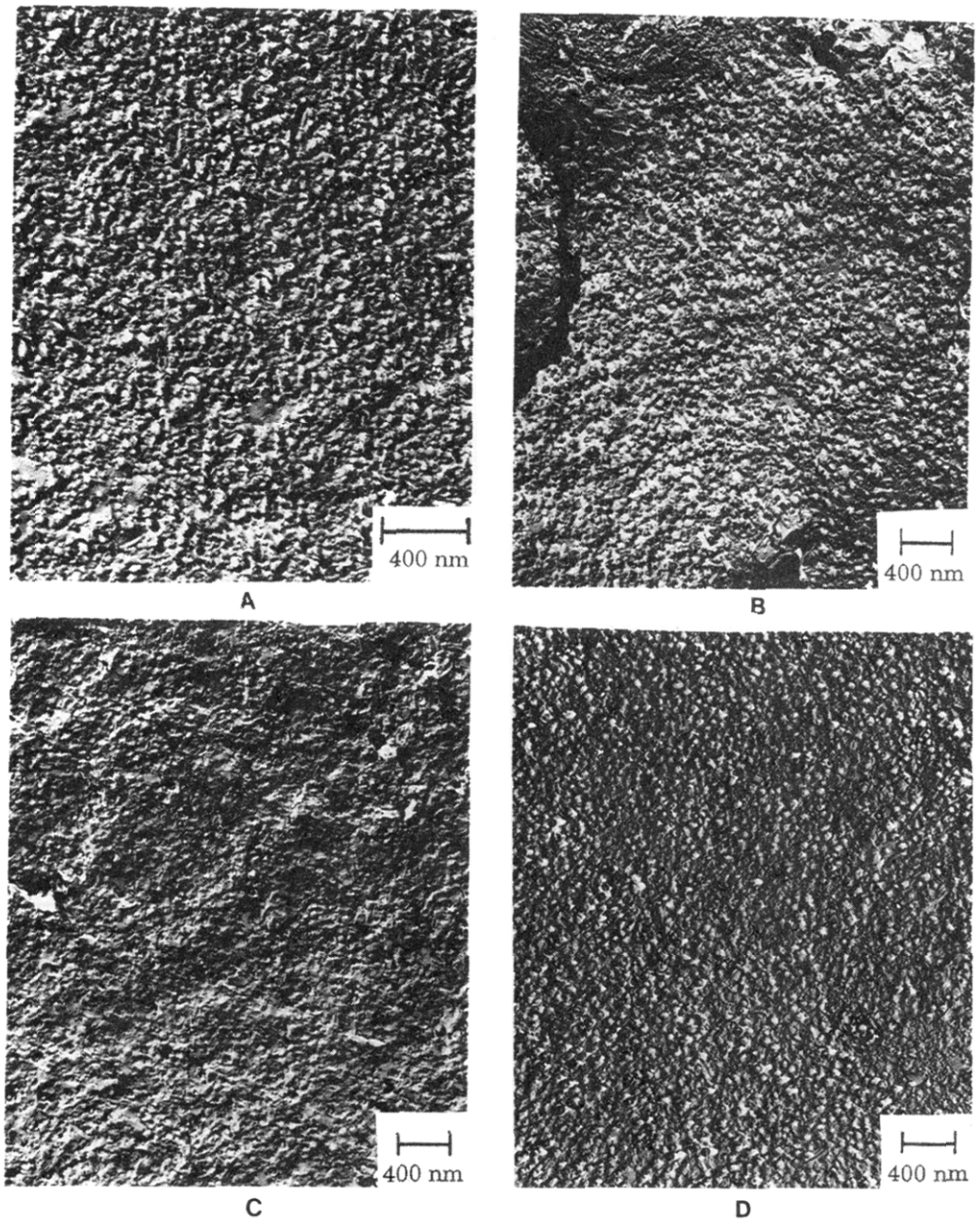

Figure 14. FFTEM images of transparent latex blend films prepared with different size ratios of hard and soft particles. D_{hard}/D_{soft} = (A) 44 nm/43 nm, (B) 110 nm/21 nm, (C) 110 nm/38 nm, and (D) 110 nm/55 nm.

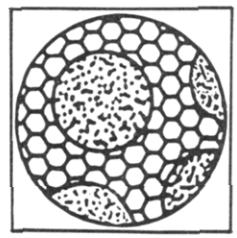

Figure 15. A model of the morphology of a clear film, showing that the hard particles are randomly dispersed and the soft particles have deformed to form a continuous matrix.

in a binary mixture of particles, A and B, the average microstructure may have either a tendency toward "dispersion", in which an A species will have on average both A and B particles as neighbors, or a tendency toward "association", in which separate clusters of A and B will form. They present evidence for the clustering of small spheres in the presence of large spheres in some samples but no sign of macroscopic fluid phase separation when the particle size ratio was not too far from unity.

From their experiments, together with the work of Biben and Hansen,[25] they suggest that when the diameter ratio of binary particles in a mixture is less than 0.2, the colloidal mixture may phase separate. This is consistent with our observations described here. We find that films prepared from mixtures of very differently sized latex particles exhibit phase separation. Our results lend support to the idea that the particle packing state in a dried latex film is largely determined by fluid phase structures in the concentrated binary dispersion during the drying process.

Surfactants play an important role in determining the structure of the concentrated dispersion. When the latex particles are covered with a layer of surfactant, the dispersion can be stable up to high solid content, and before the irreversible particle contact occurs, there is no tendency for the system to undergo spontaneous particle aggregation.[26,27] Such systems achieve a random packing of the two kinds of particles. We expect that this random arrangement persists throughout the drying process until the particles come into contact and the possibility of phase separation has been reduced.

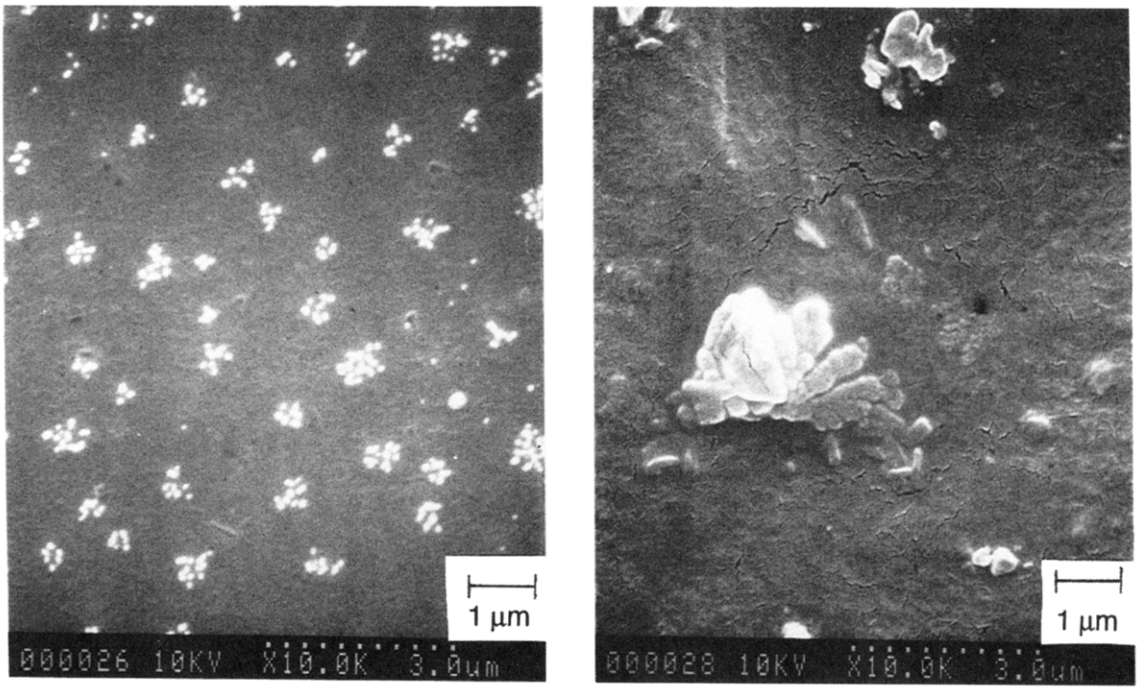

(A) (B)

Figure 16. Redistribution of particles for a blend film after annealing under different conditions: (A) 100 °C, 2 h; (B) 140 °C, 16 h. The film was prepared with D_{hard}/D_{soft} = 110 nm/55 nm, V_{hard}/V_{soft} = 1, and $T_{g,soft}$ = 5.1 °C.

When the latex is cleaned to remove all surfactant, there will still be a residual repulsive interaction between the particles resulting from the ionic initiator located at the particle surfaces. However, the surfaces of both particles have now been modified. Removal of the surfactant changes the surface tension of the particles and lowers their Coulombic repulsion. The dispersion has an enhanced tendency to flocculate not only because of the reduced Coulombic repulsion, but the surface tension of the particles no longer matches that of the aqueous medium.[3,28]

The Drying Process. Our latex dispersions dry as a propagating drying front, as depicted in Figure 7. In the surfactant-containing dispersions we examine here, we always obtain films having a thicker edge and a thinner central region. An example of such film dimensions is presented in Figure 7B. This can only be explained by assuming that the particles move from the center toward the edge and accumulate at the periphery of the drop during water evaporation. In other words, as the drying front propagates inward, it is accompanied by a net flux of latex from the wet center toward the edges of the pool.

Fluxes are not often discussed in the context of the drying process for latex dispersions. The first mention of these fluxes is due to Voyutskii and Panich,[7,29] who studied natural rubber dispersions by optical microscopy. They proposed that the globules moved from the edges of the drop being dried to the center of the section wetted with the liquid, captured by flow streams in the medium. It would be useful to repeat these experiments in our system, but our latex particles are too small to study by optical microscopy.

Recently, a detailed investigation of the drying process by optical microscopy was reported by Denkov et al.[23] for dilute dispersions of polystyrene microspheres. They found that for a convex-shaped drop placed on glass substrate, evaporation of water was accompanied by motion of the particles from the center toward the boundary of the drop. As a consequence, fewer particles remained in the central part of system. Under some circumstances, the flows were sufficiently strong to create a thicker layer at the edge of the film. Our observations of film formation, particularly of film formation from surfactant-containing systems, are consistent with their findings. When Denkov et al.[23] examined a droplet with a concave liquid layer, formed by placing the dispersion droplet inside a Teflon ring, they found that particle motion occurred in the opposite direction. An explanation in terms of surface energies and positive- and negative-curving menisci is provided in their paper.

Joanicot et al.[30] have reported that their surfactant-free dispersions dry differently from corresponding dispersions containing surfactant. Their surfactant-free dispersions dry uniformly over the surface, with no propagating drying front. In our cases, dispersions in which surfactant is removed by ion exchange also dry with a propagating drying front. Interestingly, films formed with a moving front from these surfactant-free dispersions have thicknesses that are more uniform, as measured by a micrometer. The reason for the uniform drying observed by Joanicot et al. would be that their surfactant-free dispersions contained monodispersed particles which ordered into a crystalline phase throughout the drying process, and hence the directional particle motion would be possibly suppressed. Our small soft latex particles have a broader size distribution and show an increase in size polydispersity upon washing with ion-exchange resin. It is unlikely that these particles will form a stable crystalline structure in dispersion. Clearly, the binary dispersions will not order at all.

Morphology Evolution upon Annealing. The preceding discussion treats the latex film morphology as though it is fixed at close contact and that no subsequent rearrangement can occur. One reason we

chose the T_g of the soft component as a variable was to look for morphology evolution in the film. Another way to accelerate changes within the film is through annealing. We have carried out a limited number of experiments involving sample annealing at 100 °C, just below the T_g of the PMMA microspheres, and at 140 °C, above its T_g.

Upon annealing at 100 °C for 2 h, we see for the film of D_{hard}/D_{soft} = 110 nm/55 nm and V_{hard}/V_{soft} = 1/1 (very similar to the sample in Figure 9A) that the population of hard particles on the film surface becomes much smaller, probably due to the preference of the soft polymer to move to the surface. Interestingly, the hard particles remaining on the surface tend to form small clusters but do not undergo fusion (Figure 16A). Here the annealing temperature was not high enough to allow the hard particles (T_g = 105 °C) to deform or to fuse with each other. When a similar film was annealed at 140 °C for 16 h, we observed that the hard particles had coalesced, forming clusters up to several microns in size (Figure 16B). These films exhibited varying degrees of turbidity.

We also note in passing that there are occasions in which aggregation of the hard particles in films can occur in the SEM. This seems to be caused by radiation damage, presumably to the lower T_g component of the mixture.

From these experiments we learn that while initial film morphology is dominated by processes that occur in the dispersion, the film that is produced can rearrange, and phase separation of the components can occur. From a practical point of view, one ought to be able to suppress this rearrangement by cross-linking the continuous low-T_g phase subsequent to film formation. Some current coatings technologies make use of this concept.

Conclusion

Polymer blend films were prepared by air-drying of dispersions containing mixtures of hard and soft latex particles. At least one soft latex is required so that a coherent film can be formed at room temperature. In the film the soft latex serves as a binder for the high-T_g latex. Images by FFTEM and SEM show that in these films the soft particles undergo complete coalescence, while the hard particles remain spherical in shape and are surrounded by the deformed soft particles after film drying. When the hard particles are very uniformly distributed in the soft polymer matrix, the films are transparent; when they aggregate, turbid films are obtained. The factors that affect film clarity appear to operate in the concentrated dispersion before the particles are forced into close contact by evaporation of water.

Acknowledgment. The authors thank the Institute for Chemical Sciences and Technology, as well as NSERC Canada, for their support of this research.

References and Notes

(1) Paul, D. R.; Newman, S. *Polymer Blends*; Academic Press: New York, 1978; Vols. 1–2.
(2) Miles, I. S. *Multicomponent Polymer Systems*; Burnt Mill: Harlow, 1992.
(3) Patton, T. L. *Paint Flow and Pigment Dispersion*; Wiley-Interscience: New York, 1979; p 239.
(4) Karsa, D. R. *Additives for Water-based Coatings*; Royal Chemical Society: London, 1990.
(5) (a) Roulstone, B. J.; Wilkinson, M.; Hearn, J.; Wilson, A. *J. Polym. Int.* **1991**, *24*, 87. (b) Roulstone, B. J.; Wilkinson, M.; Hearn, J. *J. Polym. Int.* **1992**, *27*, 43.
(6) Wang, Y.; Kats, A.; Juhue, D.; Winnik, M. A.; Shivers, R.; Dinsdale, C. *Langmuir* **1992**, *8*, 1435.
(7) Voyutskii, S. S. *Autohesion and Adhesion of High Polymers*; Wiley-Interscience: New York, 1963.
(8) Bradford, E. B.; Vanderhoff, J. W. *J. Macromol. Chem.* **1966**, *1*, 335.
(9) ASTM D4946-89, "Standard Test Method for Blocking Resistance of Architectural Paints", ASTM, Philadelphia, PA 19103.
(10) Winnik, M. A.; Wang, Y.; Haley, F. *J. Coat. Technol.* **1992**, *6*(811), 51–61.
(11) Friel, J. European Patent Application, 0 466 409 A1, 1992.
(12) Van den Hul, H. J.; Vanderhoff, J. W. *J. Colloid Interface Sci.* **1968**, *28*, 336.
(13) Van den Hull, H. J.; Vanderhoff, J. W. *Br. Polym. J.* **1970**, *2*, 121.
(14) Kim, H.; Wang, Y.; Winnik, M. A. *Polymer* **1994**, *35*, 1779.
(15) Bohn, L. *Polymer Handbook*, 2nd ed.; Brandrup, J., Immergut, E. H., Eds.; Wiley-Interscience: New York, 1975; P III-211.
(16) Rosen, S. L. *Polym. Eng. Sci.* **1967**, *7*(2), 115.
(17) Mark, H. F.; Bikales, N. M.; Overberger, C. G.; Menges, G. *Encyclopedia of Polymer Science and Engineering*; John Wiley and Sons: New York, 1985; Vol. 1.
(18) Vanderhoff, J. W. *Br. Polym. J.* **1970**, *2*, 161.
(19) (a) Zhao, C. L.; Holl, Y.; Pith, T.; Lambla, M. *Colloid Polym. Sci.* **1987**, *265*, 823. (b) Zhao, C. L.; Holl, Y.; Pith, T.; Lambla, M. *Br. Polym. J.* **1989**, *21*, 155.
(20) (a) Urban, M.; Evanson, K. W. *Polym. Commun.* **1990**, *31*, 279. (b) Thorstenson, T.; Urban, M. *J. Appl. Polym. Sci.* **1993**, *47*, 1387. (c) Thorstenson, T.; Tebelius, L.; Urban, M. *J. Appl. Polym. Sci.* **1993**, *49*, 103. (d) Thorstenson, T.; Tebelius, L.; Urban, M. *J. Appl. Polym. Sci.* **1993**, *50*, 1207.
(21) Henson, W. A.; Taber, D. A.; Bradford, E. B. *Ind. Eng. Chem.* **1953**, *45*, 735.
(22) Israelachvili, J. N. *Intermolecular and Surface Forces*; Academic Press: London, 1985.
(23) Denkov, N. D.; Velev, O. D.; Kralchevsky, P. A.; Ivanov, I. B.; Yoshimura, H.; Nagayama, K. *Langmuir* **1992**, *8*, 3183.
(24) Bartlett, P.; Ottewill, R. H. *Langmuir* **1992**, *8*, 1919.
(25) Biben, T.; Hansen, J. P. *Phys. Rev. Lett.* **1991**, *66*, 2215.
(26) Voyutskii, S. S. *J. Polym. Sci., Part A* **1958**, *32*, 528.
(27) Crowley, T.; Sanderson, A.; Morrison, J.; Barry, M.; Morton-Jones, A. J.; Rennie, A. R. *Langmuir* **1992**, *8*, 2110.
(28) Buechler, P. R. *J. Paint Technol.* **1973**, *45*(577), 60–64.
(29) Voyutskii, S. S.; Panich, R. M.; Kal'yanova, K. A. *Kolloid. Zh.* **1951**, *13*, 89.
(30) Joanicot, M.; Wong, K.; Maquet, J.; Chevalier, Y.; Pichot, C.; Graillat, C.; Lindner, P.; Rios, L.; Cabane, B. *Prog. Colloid Polym. Sci.* **1990**, *81*, 175.

MA950636O